Glia-Like Cells from Late-Passage Human MSCs Protect Against Ischemic Stroke Through IGFBP-4

Jeong-Woo Son[1] · Jihye Park[2] · Ye Eun Kim[1,3] · Jieun Ha[2] · Dong Woo Park[4] · Mi-Sook Chang[2,5] · Seong-Ho Koh[1,3]

Abstract

Stem cell therapy is considered to be a promising future treatment for intractable neurological diseases, although all the clinical trials using stem cells have not yet shown any good results. Early passage mesenchymal stem cells (MSCs) have been used in most clinical trials because of the issues on safety and efficacy. However, it is not easy to get plenty of cells enough for the treatment and it costs too much. Lots of late passage MSCs can be obtained at lower cost but their efficacy would be a big hurdle for clinical trials. If late passage MSCs with better efficacy could be used in clinical trials, it could be a new and revolutionary solution to reduce cost and enhance easier clinical trials. In the present study, it was investigated whether late passage MSCs could be induced into glia-like cells (ghMSCs); ghMSCs had better efficacy and they protected neurons and the brain from ischemia, and insulin-like growth factor binding protein-4 (IGFBP-4) played a critical role in beneficial effect of ghMSCs. ghMSCs were induced from MSCs and treated in in vitro and in vivo models of ischemia. They effectively protected neurons from ischemia and restored the brain damaged by cerebral infarction. These beneficial effects were significantly blocked by IGFBP-4 antibody. The current study demontsrated that late passage hMSCs can be efficiently induced into ghMSCs with better neuroprotective effect on ischemic stroke. Moreover, the results indicate that IGFBP-4 released from ghMSCs may serve as one of the key neuronal survival factors secreted from ghMSCs.

Keywords Cell death · Growth factor · Ischemia · Mesenchymal stem cells · Neuronal protection

---

Jeong Woo Son and Jihye Park contributed equally to this work.

✉ Mi-Sook Chang
  mschang@snu.ac.kr

✉ Seong-Ho Koh
  ksh213@hanyang.ac.kr

1   Department of Neurology, Hanyang University College of Medicine, Gyeongchun-ro, Guri-Si11923Gyeonggi-do, Republic of Korea

2   Laboratory of Stem Cell & Neurobiology, Department of Oral Anatomy, Dental Research Institute and School of Dentistry, Seoul National University, Seoul 03080, Republic of Korea

3   Department of Translational Medicine, Hanyang University Graduate School of Biomedical Science & Engineering, Gyeongchun-ro, Guri-Si 11923, Gyeonggi-do, Republic of Korea

4   Department of Radiology, Hanyang University College of Medicine, Seoul 04763, Republic of Korea

5   Neuroscience Research Institute, Seoul National University, Seoul 03080, Republic of Korea

Introduction

Countless intractable neurological diseases are caused by nervous system damage. Stem cells from various sources are considered a promising treatment for intractable neurological diseases due to their ability to replace lost or damaged cells in the nervous system [1]. Previous studies have reported that embryonic stem cells (ESCs) and induced pluripotent stem cells (iPSCs) can be differentiated into diverse neuronal cells and replace the damaged nervous system. However, these cells are barred from use in clinical trials because of safety issues that may produce undesirable tumors [2–4]. Therefore, most ongoing clinical trials utilize adult stem cells, especially early-passage human mesenchymal stem cells (hMSCs), which exhibit better paracrine effects based on their secreted factors [5].

Several previous studies have shown that late-passage adult stem cells are much less protective toward the damaged nervous system than early-passage cells regardless of the number of transplanted cells. One reason is that later-passage adult stem cells secrete lower amounts of growth factors and/or cytokines [6]. In addition, late-passage adult stem cells also possess lower potential for differentiation and migration than

early-passage cells, which makes early-passage cells more beneficial [7]. However, obtaining sufficient numbers of early-passage cells for clinical trials can be difficult [8].

This study aimed to demonstrate that late-passage hMSCs could be induced into ghMSCs with enhanced paracrine activity. Through the use of in vitro and in vivo ischemic stroke models, this study also investigated whether the induced ghMSCs were more neuroprotective than hMSCs through protective mechanisms modulated by insulin-like growth factor-binding protein-4 (IGFBP-4), which is known to be one of six IGFBPs that modulate IGF signaling by either enhancing or inhibiting the diffusion of IGF [9].

Materials and Methods

hMSC Culture

Adult hMSCs isolated from normal human bone marrow (Cambrex Bioscience, Walkersville, MD, USA) were cultured in low-glucose Dulbecco's modified Eagle's medium (DMEM) supplemented with 10% fetal bovine serum (FBS; Gibco, Waltham, MA, USA). Cells (passages 6–12) were cultured at 37 °C with 5% CO_2.

Primary Cortical Neuron-Enriched Cultures and OGD Treatment

All procedures involving animals were approved by the Institutional Animal Care and Use Committee, Seoul National University (Seoul, Republic of Korea). Primary cortical neuron-enriched cultures were prepared according to a previously described method [10]. In brief, cerebral cortices were obtained from E17 SD rat embryos. The dissociated cells were seeded at 7.5×10^4 cells/cm^2 on 50 μg/ml PDL- and 5 μg/ml laminin-coated plates in Neurobasal-A Medium (NB; Gibco) supplemented with 10% FBS. The medium was replaced with NB supplemented with 2% B27 (Gibco) after 24 h. The primary cortical neuron-enriched cultures were refreshed every 3 or 4 days.

To induce OGD, cortical neurons were rinsed twice with phosphate-buffered saline (PBS; pH 7.4) and 95% N_2; 5% CO_2 gas mixture-injected glucose-free DMEM (OGD media) was added. Then, cells were placed in a humidified chamber, subjected to a deoxygenated atmosphere (95% N2, 5% CO_2) and kept in a 37 °C incubator for 3 h. OGD was terminated by replacing the culture media, followed by reoxygenation in a 37 °C incubator with 5% CO_2 for 24 h, except for western blot analysis of pAkt expression.

Glia-Like Cell Induction of hMSCs (ghMSCs)

Glia-like cells were induced from hMSCs according to a previously described protocol [11]. Briefly, hMSCs were treated with 1 mM β-mercaptoethanol (Sigma-Aldrich, St Louis, MO, USA) for 24 h. Then, the cells were treated with 0.28 μg/mL all-trans-retinoic acid (Sigma-Aldrich) for 3 days and with a cocktail containing 10 ng/mL bFGF, 5 ng/mL PDGF-AA (both from PeproTech, Rocky Hill, NJ, USA), 10 μM forskolin (Sigma-Aldrich), and 200 ng/mL HRG-β1 (R&D Systems, Minneapolis, MN, USA) for 8 days.

Conditioned Media (CM) and Reagent Treatment

hMSCs and ghMSCs (1×10^4 cells/cm^2) were rinsed twice with PBS and incubated in serum-free NB for 18 h. The collected media was added to the OGD-treated primary cortical neuron-enriched cultures.

The reagents were preincubated in ghMSC-CM under the following conditions: 40 μg/ml IGFBP-4 antibody (anti-BP-4; R&D Systems) [12], 50 μM PD98059 (Promega Corp., Madison, WI, USA), 100 nM wortmannin (Sigma-Aldrich), 500 nM picropodophyllin (PPP; Santa Cruz Biotechnology, Santa Cruz, CA, USA), or recombinant human IGFBP-4 (rhBP-4; PeproTech) for 30, 15, 30, 15, or 30 min, respectively [10]. OGD-treated primary cortical neuron-enriched cultures were incubated in prepared ghMSC-CM.

Animals and Induction of Middle Cerebral Artery Occlusion (MCAo)

All animal procedures were performed in accordance with the Hanyang University guidelines for the care and use of laboratory animals and were approved by the Institutional Animal Care and Use Committee (IACUC) of Hanyang University. In accordance with Animal Research: Reporting of In vivo Experiments (ARRIVE) guidelines, all experiments were carried out in a strictly blinded fashion; inclusion and exclusion criteria were predetermined, and attrition due to mortality and other causes was reported. Adult male SD rats weighing 270–300 g were used (Orient Bio, Seoul, Korea). After a 7-day period of adaptation and pretraining for neurological examination, the left middle cerebral artery (MCA) of SD rats was occluded for 2 h using the intraluminal filament technique as described previously [13–15]. The rats were anesthetized with isoflurane (3% for induction and 2% for surgical procedures) in a mixture of 30% oxygen and 70% nitrous oxide. Body temperature was maintained at 36.6 ± 0.5 °C with a thermistor-controlled heating pad. Arterial pH, pCO_2, pO_2, and hematocrit were measured in 0.1 ml of arterial blood obtained from a right femoral catheter using a blood analysis system (International Technidyne, Edison, NJ, USA). Arterial pressure was monitored from the femoral catheter using a

strain gauge transducer (LIFE KIT DX-360; Nihon Kohden, Tokyo, Japan) and amplifier (MacLab Bridge Amplifier, AD Instruments Pty Ltd., Castle Hill, Australia). Phasic pressure, mean arterial pressure (MAP), and heart rate (HR) were recorded at a sampling rate of 200/s using a data acquisition system and laboratory computer (MacLab 8 analog-to-digital converter and Macintosh computer). After 2 h of occlusion, reperfusion was performed as described previously [10]. A sham surgery was performed by introducing and then immediately withdrawing a thread into the left common carotid artery. Other procedures for the sham surgery were identical those for transient MCAo. We measured regional cerebral blood flow (rCBF) using a laser Doppler flowmeter (ALF21; Advance, Tokyo, Japan) and a wire-type probe (0.3 mm in diameter; Unique Medical, Tokyo, Japan), which were inserted through a small-burr hole just 2 mm lateral to the bregma at the surface of the cortex to evaluate the ischemic core in the caudate and putamen.

Experimental Procedure for Cell Transplantation

To evaluate the effect of cell treatments on cerebral infarction, SD rats with cerebral infarction were divided into four groups. The first group was used as the control; the second group was treated with hMSCs; the third group was treated with ghMSCs, and the last group was treated with a combination of ghMSCs and anti-BP-4 (100 μg/ml). In total, 2×10^5 cells were suspended in 10 μl of neurobasal media and transplanted into the side of the brain (AP = − 2, L = 2, V = 2) contralateral to the cerebral infarction in each group ($n = 10$).

Cell Viability Assay

Cell viability after treatment was analyzed using an MTT (3-(4,5-dimethylthiazol-3-yl)2,5-diphenyl tetrazolium bromide; Sigma-Aldrich) assay. MTT was added at a final concentration of 1 mg/ml to neurons cultured in 4-well plates and incubated for 1 h at 37 °C. The MTT solution was carefully aspirated, and formazan crystals were dissolved in 130 μl of dimethyl sulfoxide (DMSO). The optical density was measured at 554 nm on a microplate reader (Fluostar Optima, BMG Labtech, Cary, NC, USA).

In Vivo MRI Study

All MR images were obtained using a 3-Tesla MR machine (Achieva; Philips, Best, The Netherlands) with a 47-mm ds microscopy coil (mouse coil; Invivo Corporation, Gainesville, FL, USA). All rats underwent multiplanar gradient recalled acquisition in the steady state (MPGR) coronal imaging (TR/TE = 596/16 ms, slice thickness/gap = 0.7/0 mm, matrix = 132 × 129, FOV = 39 × 39 mm) at different time points after stereotaxic surgery. MPGR coronal imaging was performed 1 day after transient MCAo to confirm the existence of cerebral infarction and 4 weeks after transplantation to assess the effect of each condition on cerebral infarction. During the interval, neurobehavioral functions were evaluated on a regular basis. The rats were then sacrificed, and the brains were used for the molecular biological assessment.

Neurobehavioral Function Test

A modified neurological severity score (mNSS) was blindly a before transient MCAo, before reperfusion, and before and after cell transplantation. mNSS is based on consciousness (0, normal; 1, restless; 2, lethargic; 3, stuporous), gait (0, normal; 1, paw adduction; 2, unbalanced walking; 3, circling; 4, unable to stand; 5, no movement), and limb tone (0, normal; 1, spastic; 2, flaccid). Neurological function was graded on a scale of 0 to 10 (normal score, 0; maximal deficit score, 10) [16]. The distribution of rats was based on mNSS and MRI data analysis measured 1 day after transient MCAo.

Long-Term Neurological Outcome

Long-term neurological outcome was investigated as follows: sensorimotor function was assessed using beam-walking and modified sticky-tape tests performed before transient MCAo and at 7, 14, 21, and 28 days after transplantation by an investigator who was blinded to the experimental groups. For the beam-walking test, rats were trained 3 days before MCAo to walk on a wooden beam (2.5 × 2.5 × 80 cm), 60 cm above the floor to return to their home cage. The test was scored as follows: 0, traverses the beam with no foot slip; 1, traverses by grasping the lateral side of the beam; 2, shows disability walking on the beam but can traverse; 3, takes a considerable amount of time to traverse the beam because of difficulty walking; 4, is unable to traverse the beam; 5, is unable to move the body or any limb on the beam; and 6, is unable to stay on the beam for 10 s [17]. For the modified sticky-tape test, a sleeve was created using a 3-cm piece of green paper tape, 1 cm in width, and was wrapped around the forepaw so that the tape attached to itself and the fingers protruded slightly from the sleeve. The typical response was for the rat to vigorously attempt to remove the sleeve by either pulling at the tape with its mouth and/or brushing the tape with its contralateral paw. After attachment of the sleeve, the rat is placed in its cage and observed for 30 s. The timer was turned on only while the animal attempted to remove the taped sleeve. The data collected represent the fraction of the 30-s observation period that the animal spent attending to the stimulus. The contralateral and ipsilateral limbs were tested separately. The test was repeated three times per test day, and the best two scores were averaged [18]. Motor test data are presented as the mean duration (seconds) and right/left ratio.

Western Blotting

Cells were rinsed twice with cold PBS and incubated in RIPA buffer (50 mM Tris-HCl, pH 7.4, 1% NP40, 0.25% sodium deoxycholate, 150 mM NaCl, 1 mM Na_3VO_4, 0.2 mg/ml leupeptin, 0.2 mg/ml aprotinin, 0.1 M PMSF, and 0.5 M sodium fluoride) on ice. Following lysate centrifugation, the supernatants were separated via sodium dodecyl sulfate-polyacrylamide gel electrophoresis (SDS-PAGE). Primary antibodies against Akt (Cell Signaling, Beverly, MA, USA), pAkt (Cell Signaling), Bax (BD Pharmingen, San Jose, CA, USA), COX IV (Cell Signaling), and α-tubulin (Sigma-Aldrich) were diluted in 3% BSA blocking solution at 1:1000. After incubation with goat-anti-rabbit or goat-anti-mouse horseradish peroxidase-conjugated secondary antibody (1:5000; Sigma-Aldrich), targeted antigens were detected using a western blot detection kit (Thermo Fisher Scientific, Inc.). Mitochondrial and cytosolic fractions were isolated using a Mitochondrial Fraction kit (Active Motif, Carlsbad, CA, USA) based on the manufacturer's instructions.

Rats from each group were sacrificed following isoflurane anesthesia. The brains were perfused with PBS and stored at − 80 °C. Then, the frozen brain tissues were rapidly microdissected on an ice-chilled plate. The tissues were incubated in RIPA II cell lysis buffer (100 mM Na_3VO_4, 100 mM PMSF, 100 mM NaF, and protease inhibitor) and homogenized with a Q55 sonicator (Qsonica, Melville, NY, USA). Equal amounts (40 μg) of protein were separated for 25 min via 12% SDS-PAGE and transferred to nitrocellulose membranes for 1 h 30 min. Primary antibodies against Akt (1:500), ERK (1:500; Cell Signaling), NeuN (1:200; Abcam, UK), Bax (1:500; Cell Signaling), pAkt (1:200), p-ERK (1:500; Cell Signaling), and cleaved caspase-9 (1:500; Cell Signaling) were diluted in 2% skim milk blocking buffer. After incubation with anti-rabbit or anti-mouse horseradish peroxidase-

conjugated secondary antibody (1:2000; Amersham Pharmacia Biotech, Piscataway, NJ, USA), targeted antigens were detected using a mixture of solution A and solution B (West-Q Chemiluminescent Substrate Kit, GenDEPOT).

Quantitative Real-Time PCR

Total RNA was extracted using TRIzol reagent (Invitrogen, Carlsbad, CA, USA), followed by DNase treatment. Reverse transcription to cDNA was performed using M-MLV reverse transcriptase (Promega) at 42 °C for 1 h. cDNA was amplified using SYBR FAST qPCR Kits (KAPA Biosystems) with gene-specific primers (Table 1). The expression level of each target gene was normalized to GAPDH and analyzed using the comparative Ct method. The ΔCt value is determined by subtracting the Ct values; the cycle number at the threshold: [ΔCt = Ct (Target) − Ct (GAPDH)]. The relative value of the target gene to endogenous GAPDH was determined as the fold-change in GAPDH = $2^{-\Delta Ct}$.

Immunohistochemistry

The cultures were fixed with 4% paraformaldehyde (PFA) in PBS and incubated in blocking solution containing 5% normal goat serum and 0.1% Triton-X100 in PBS. The cells were incubated overnight with primary antibodies against GFAP (1:200; Merck Millipore) and S100 (1:250; Dako) diluted in blocking solution at 4 °C. After several washes in PBS, cells were incubated for 1 h at room temperature with the following secondary antibodies: Alexa Fluor® 488 anti-mouse IgG (Molecular Probes) and Alexa Fluor® 546 anti-rabbit IgG (Molecular Probes). Then, cells were counterstained with 4,6-diamidino-2-phenylindole (DAPI) (Santa Cruz Biotechnology) and examined under a digital inverted fluorescence microscope (DM5000B; Leica).

Table 1 Real-time PCR primer pairs

Gene name	Forward primer sequence	Reverse primer sequence	Product size (bp)	GenBank accession
GAPDH	GTCAGTGGTGGACCTGACCT	CACCACCCTGTTGCTGTAGC	256	NM_001256799
GFAP	CAACCTGCAGATTCGAGAAA	GTCCTGCCTCACATCACATC	153	NM_002055
IGFBP-4	GCCCAAGAGGACTGAGACTG	CACATGCCAAAATCAGAGGA	200	NM_001552.2
Nestin	CACCTGTGCCAGCCTTTCTTA	TTTCCTCCCACCCTGTGTCT	170	NM_006617
PAPP-A	CAGAATGCACTGTTACCTGGA	GCTGATCCCAATTCTCTTTCA	168	NM_002581.4
Pax6	AGGTATTACGAGACTGGCTCC	TCCCGCTTATACTGGGCTATTT	104	NM_001604
PDGFRα	TACACTTGCTATTACAACCACA	ATCCTCCACGATGACTAAAT	135	NM_006206.3
SLC1A2	TGCCAACAGAGGACATCAGCCT	CAGCTCAGACTTGGAGAGGTGA	128	NM_004171.3
SLC1A3	GGTTGCTGCAAGCACTCATCAC	CACGCCATTGTTCTCTTCCAGG	95	NM_004172.4
Sox2	AGTCTCCAAGCGACGAAAAA	GCAAGAAGCCTCTCCTTGAA	141	NM_003106
Sox10	CGGACCAGTACCCGCACCT	GGCGCTTGTCACTTTCGTTCA	87	NM_006941.3
S100β	GGAGACGGCGAATGTGACTT	GAACTCGTGGCAGGCAGTAGTAA	72	NM_006272.2
Vimentin	AGAACTTTGCCGTTGAAGCTG	CCAGAGGGAGTGAATCCAGATTA	255	NM_003380

Five rats from each group were used for histological and immunohistochemical analysis. The PBS-perfused brains were also perfused with 4% PFA. Then, the brains were quickly removed, further fixed overnight in 4% PFA, and incubated in 30% sucrose solution for 3 days. Brain tissue was mounted on a cold-metal block using optimal cutting temperature (OCT) compound (Leica, Wetzlar, Germany), and then brain sections (20-μm thickness) were cut on a motorized cryostat (Leica, Wetzlar, Germany). Brain tissues were placed on a Muto Silane coating slide and treated with 3% H_2O_2 to block
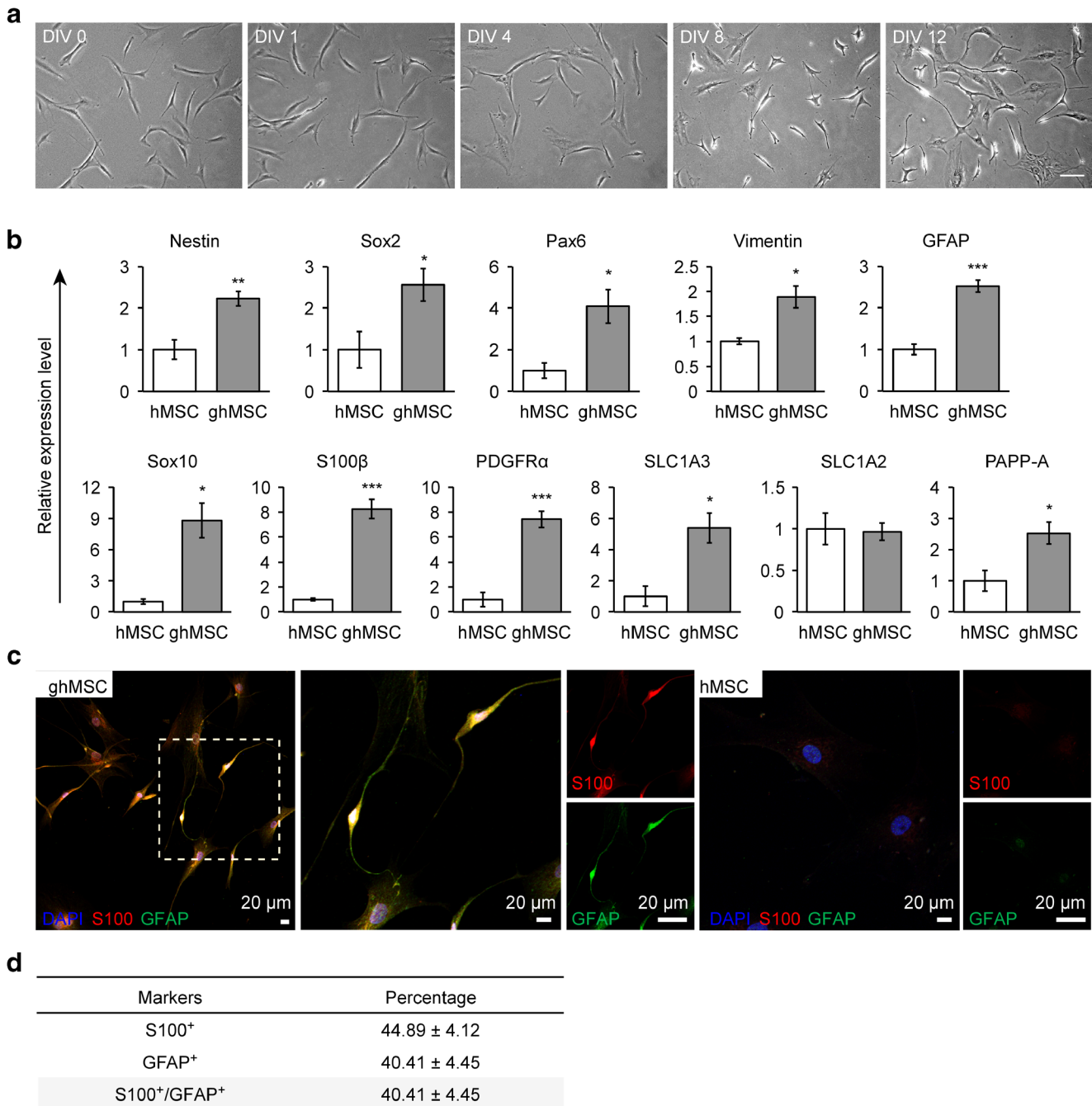
Fig. 1 Characteristics of induced glia-like hMSCs (ghMSCs). **a** Morphological changes in cells were observed using bright-field images during ghMSC induction. Scale bar 100 μm. **b** Real-time qPCR of astrocyte (GFAP, S100β, SLC1A3, SLC1A2), Schwann cell and oligodendrocyte (Sox10), and oligodendrocyte precursor markers (PDGFRα) and PAPP-A. The mRNA levels of a given gene were quantified by densitometry and normalized to the corresponding GAPDH level. *$P < 0.05$, **$P < 0.01$, ***$P < 0.001$ versus hMSCs. The data were analyzed using unpaired Student's t tests. **c** Immunocytochemistry analysis of S100 and GFAP expression levels in ghMSCs and hMSCs cultured as a monolayer on cover slips. Scale bar 20 μm. **d**) Quantitative analysis of astrocyte marker protein expression in ghMSCs from at least three different randomly chosen fields. The percentage represents cells positive for each marker over DAPI-positive cells, the total cell number (mean ± SEM)

endogenous peroxidase activity. Tissues were incubated overnight with primary antibodies diluted in 10% FBS blocking solution at 4 °C as follows: pAKT (1:500), p-ERK (1:500), cleaved caspase-3 (1:500; Cell Signaling), Bcl-xl (1:250; Cell Signaling), Bax (1:100; Abcam), cytochrome c (1:500; Santa Cruz Biotechnology), and NeuN (1:500; Millipore, MA, USA). After several washes in PBS, the tissues were incubated with 5% FBS to block unbound primary antibodies. Then, secondary antibodies conjugated to tetramethylrhodamine isothiocyanate (TRITC) (Invitrogen, Carlsbad, CA, USA) or fluorescein isothiocyanate (FITC) (Invitrogen) were applied.

The tissues were mounted with DAPI mounting solution (Vector Laboratories, H-500) and examined via fluorescence microscopy (Olympus, Center Valley, PA, USA).

Enzyme-Linked Immunosorbent Assay (ELISA)

Cells were rinsed twice with PBS and cultured in serum-free NB with additional treatment depending on the experimental condition for 30 h. The supernatant was collected and centrifuged at 1200 rpm for 5 min and analyzed using an IGF-1 or an IGF-2 ELISA kit for rat (Abcam), as well as an IGFBP-4
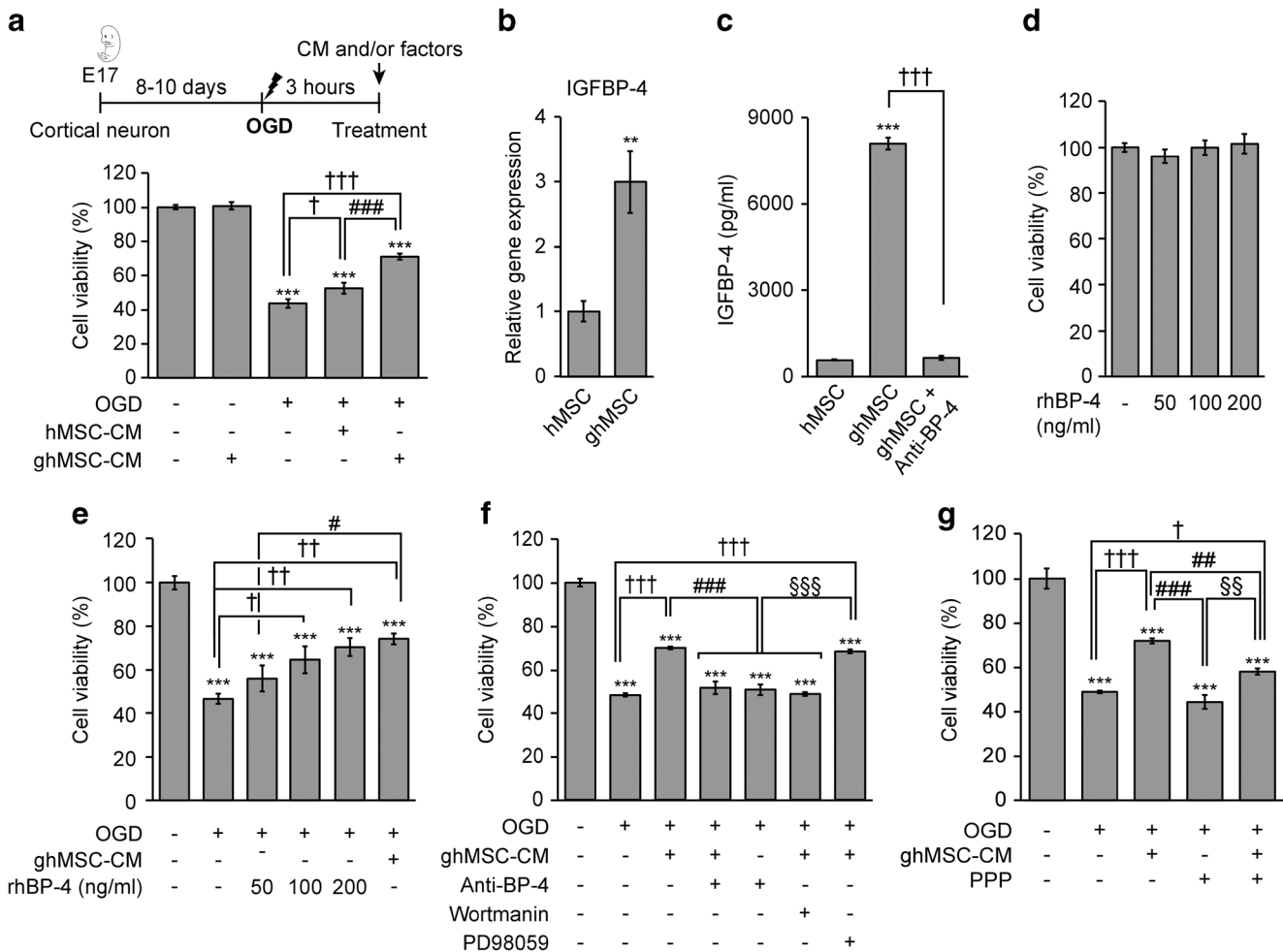
Fig. 2 Neuroprotective effect of IGFBP-4 in ghMSC-CM on OGD-treated primary cortical neurons via Akt activation. a Primary cortical neurons were treated with oxygen-glucose deprivation (OGD) for 3 h and then incubated with hMSC-CM or ghMSC-CM. ***$P < 0.001$ versus control or control (+) ghMSC-CM; $^\dagger P < 0.05$, $^{\dagger\dagger}P < 0.01$ versus OGD; $^\#P < 0.05$ versus OGD (+) hMSC-CM. (b) Quantitative real-time PCR analysis of IGFBP-4 mRNA levels in hMSCs and ghMSCs. mRNA expression levels were normalized to GAPDH. *$P < 0.05$, ***$P < 0.001$ versus control. The data were analyzed using unpaired Student's t tests. c IGFBP-4 concentrations were analyzed by ELISA in hMSC-CM, ghMSC-CM, or ghMSC-CM preincubated with anti-BP-4. ***$P < 0.001$ versus control; $^{\dagger\dagger\dagger}P < 0.001$ versus ghMSC. d e) Cortical neurons were treated with different concentrations of recombinant human IGFBP-4 (rhBP-4) (50 to 200 ng/ml) to observe its effect on cell viability

before and after OGD treatment. All MTT assays were carried out 24 h after OGD treatment. ***$P < 0.001$ versus control; $^\dagger P < 0.05$, $^{\dagger\dagger}P < 0.01$ versus OGD; $^\#P < 0.05$ versus OGD (+) 50 ng/ml rhBP-4. (f) After OGD treatment, cells were incubated with ghMSC-CM or ghMSC-CM pretreated with anti-IGFBP-4 antibody (anti-BP-4), PD98059 (50 μM), or wortmannin (100 nM). ***$P < 0.001$ versus control; $^{\dagger\dagger\dagger}P < 0.001$ versus OGD; $^{\#\#\#}P < 0.001$ versus OGD (+) ghMSC-CM; $^{\S\S\S}P < 0.001$ versus OGD (+) ghMSC-CM with PD98059. g OGD-damaged cortical neurons were treated with ghMSC-CM or neurobasal media preincubated with PPP (500 nM). ***$P < 0.001$ versus control; $^\dagger P < 0.05$, $^{\dagger\dagger\dagger}P < 0.001$ versus OGD; $^\#P < 0.05$, $^{\#\#\#}P < 0.001$ versus OGD (+) ghMSC-CM; $^{\S\S}P < 0.01$ versus OGD (+) PPP. a, c–g The data were analyzed using one-way ANOVA with post hoc Newman-Keuls test

DuoSet ELISA for human (R&D Systems), based on the manufacturer's instructions. The optical density was measured at 450 nm on a microplate reader (Epoch2, Bio-Tek, Winooski, VT, USA).

Statistical Analysis

In vitro data were analyzed using Student's *t* test, one-way analysis of variance (ANOVA) followed by Newman-Keuls post hoc testing, and two-way ANOVA followed by the Bonferroni post hoc testing using R (R Development Core Team 2010).

For statistical analyses of in vivo data, normality was tested suing the Kolmogorov-Smirnov test. All in vivo statistical analyses were performed using Student's *t* test and one-way ANOVA followed by Tukey's post hoc testing using the SPSS 17.0 software package for Windows (SPSS, Seoul, Korea).
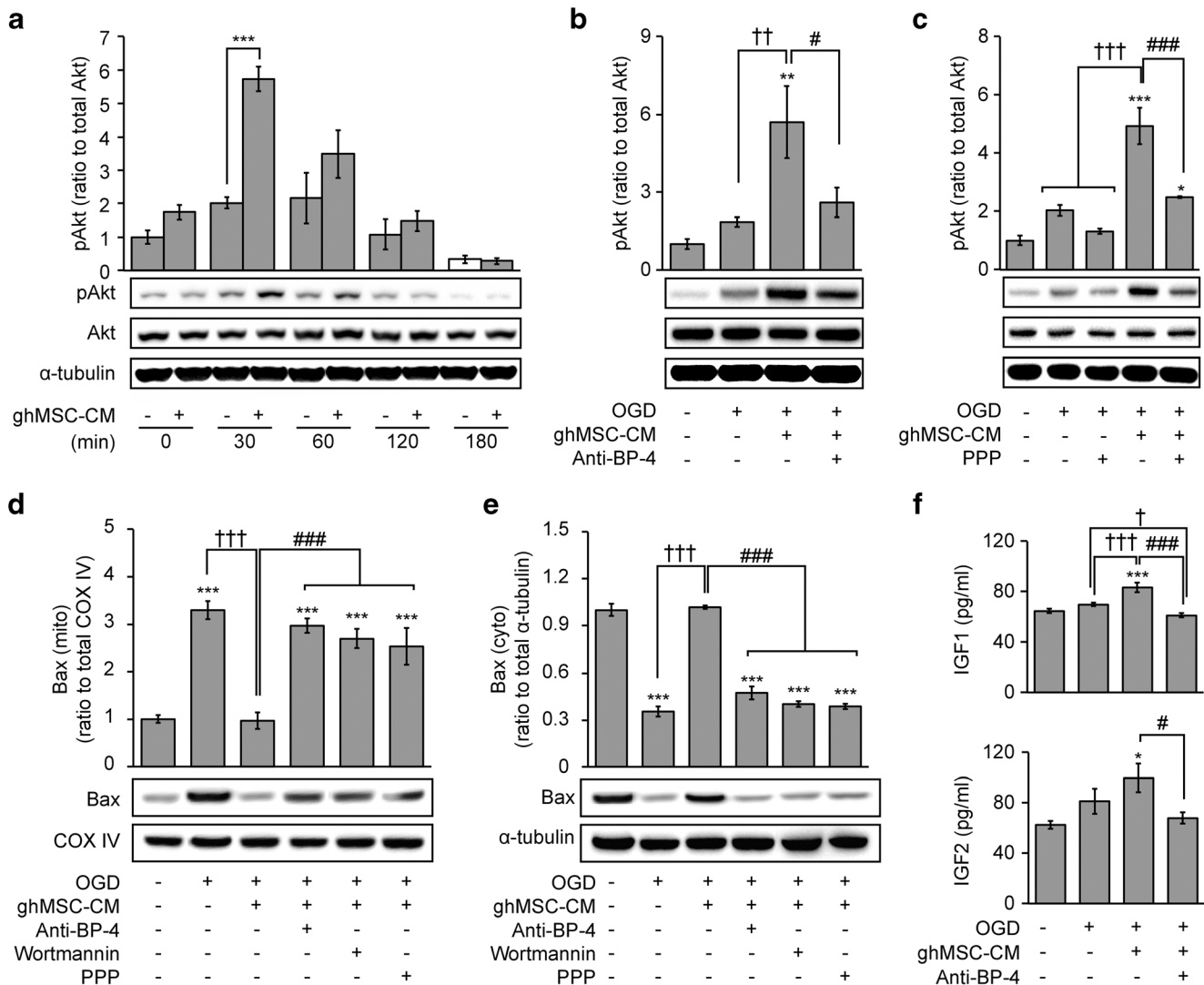
Fig. 3 IGFBP-4 modulates antiapoptotic pathways and extracellular levels of IGFs in primary cortical neurons. **a** pAkt expression levels in OGD-treated primary cortical neurons observed 30, 60, 120, and 180 min after ghMSC-CM treatment via western blotting. ***$P < 0.001$ versus control. The data were analyzed by two-way ANOVA with post hoc Bonferroni test. **b** pAkt levels were observed in primary cortical neurons incubated with ghMSC-CM or ghMSC-CM preincubated with anti-BP-4 following OGD treatment. **$P < 0.01$ versus control. ††$P < 0.01$ versus OGD; #$P < 0.05$ versus OGD (+) 50 ng/ml rhBP-4. **c** OGD-damaged primary cortical neurons were treated with ghMSC-CM preincubated with PPP (500 nM) for 15 min. *$P < 0.05$, ***$P < 0.001$ versus control; †††$P < 0.001$ versus OGD or OGD (+) PPP; ###$P < 0.001$ versus OGD (+) ghMSC-CM. pAkt expression levels were detected 30 min after OGD treatment. **d e**) Bax translocation was quantified by immunoblotting after incubation with ghMSC-CM or ghMSC-CM with anti-BP-4 following OGD treatment. Mitochondria (mito) and cytosolic (cyto) Bax levels were analyzed 24 h after OGD treatment. ***$P < 0.001$ versus control; †††$P < 0.001$ versus OGD; ###$P < 0.001$ versus OGD (+) ghMSC-CM. **f** Concentrations of IGF-1 and IGF-2 were analyzed by ELISA in the supernatant of OGD-treated primary cortical neurons incubated with ghMSC-CM or ghMSC-CM preincubated with anti-BP-4. *$P < 0.05$, ***$P < 0.001$ versus control; †$P < 0.05$, †††$P < 0.001$ versus OGD; #$P < 0.05$, ###$P < 0.001$ versus OGD (+) ghMSC-CM. **b–f** The data were analyzed by one-way ANOVA with post hoc Newman-Keuls test

All numerical results were expressed as the mean ± standard error of the mean (SEM) from three or more independent experiments, and statistical significance was set at $P < 0.05$.

Results

Induction of Late-Passage hMSCs into Glia-Like Cells

It was confirmed that late-passage hMSCs were efficiently induced into ghMSCs using the same method as previously reported by our group [11]. Untreated late-passage hMSCs showed a symmetrical flattened and fibroblast-like morphology, while ghMSCs exhibited an elongated bipolar and glia-like morphology following exposure to induction media (Fig. 1a). In this study, we further established a method involving cryopreservation of ghMSCs in the middle of induction and subsequent induction using cryopreserved cells. The cryopreservation did not alter the adopted morphological and molecular features (data not shown).

Real-time quantitative PCR (qPCR) analysis of radial glial markers such as Nestin, Sox2, Pax6, Vimentin, and GFAP revealed that ghMSCs acquired astrocyte- or oligodendrocyte-like molecular features (Fig. 1b). We next sought to investigate the mRNA expression levels of additional glial markers. Real-time qPCR analysis showed that genes associated with astrocytes (GFAP, S100β, SLC1A3 (GLAST)), Schwann cells/oligodendrocytes (Sox10), and oligodendrocyte precursors (PDGFRα) were significantly increased in ghMSCs compared with hMSCs (Fig. 1b). In addition, we examined the mRNA levels of pregnancy-associated plasma protein-A (PAPP-A), a major IGFBP-4 and IGF complex protease, which might play an important role in the IGFBP-4 and IGF-1 system under ischemic conditions [19]. PAPP-A mRNA expression levels were clearly enhanced by up to 2.5-fold ($P < 0.05$) in ghMSCs compared with the control (Fig. 1b). Immunocytochemistry analysis confirmed that the glial markers S100 and GFAP were expressed in approximately 45% and 40% of total ghMSCs, respectively, while these proteins were barely expressed in control hMSCs (Fig. 1c). Taken together, these findings suggest that the previously reported induction protocol [20] can generate other types of glia-like cells, as well as Schwann cell-like cells, from hMSCs.

Neuroprotective Effect of IGFBP-4 Released from ghMSCs in OGD-Treated Primary Cortical Neurons

Here, we sought to investigate the neuroprotective effect of late-passage hMSC-conditioned media (hMSC-CM) and ghMSC-CM in oxygen-glucose deprivation (OGD)-treated rat primary cortical neuron cultures. Compared with control hMSC-CM, ghMSC-CM significantly enhanced cell survival in OGD-treated cortical neurons (Fig. 2a). We previously found that ghMSCs secreted significantly higher levels of IGFBP-4 than hMSCs using a human growth factor array [11]. Therefore, we next examined the neuroprotective effect of IGFBP-4 released from ghMSCs. Consistent with the previous study [11], IGFBP-4 mRNA levels in ghMSCs were significantly enhanced by up to threefold ($P < 0.01$) compared with control hMSCs (Fig. 2b). Moreover, an enzyme-linked immunosorbent assay (ELISA) revealed significantly increased IGFBP-4 levels in ghMSC-CM, which were blocked by a neutralizing antibody against IGFBP-4 (anti-BP-4) (Fig. 2c). To examine whether IGFBP-4 itself induced neuroprotection, OGD-damaged cortical neurons were treated with different concentrations of recombinant human IGFBP-4 (rhBP-4). Higher concentrations of IGFBP-4 showed increased protection of OGD-damaged cortical neurons without any effect on cell viability ($P < 0.01$) (Fig. 2d, e). Interestingly, anti-BP-4 abolished the neuropro MCAo tective effect of ghMSC-CM, whereas anti-BP-4 itself showed no effect on cell survival ($P < 0.001$) (Fig. 2f).

To identify IGFBP-4-mediated signal transduction in neuronal protection by ghMSC-CM, two different pathways, the phosphoinositide 3-kinase (PI3K)/Akt and extracellular signal-regulated kinase (ERK) pathways, which are involved in IGF signaling, were investigated. Wortmannin, an inhibitor of PI3K/Akt, eliminated the ghMSC-CM-mediated neuroprotection of OGD-treated primary cortical neurons ($P < 0.001$) (Fig. 2f). However,

Fig. 4 Effect of ghMSCs on cerebral infarction and its blockade by anti-BP-4. **a** Schematic illustration of the in vivo studies. The middle cerebral artery (MCA) of SD rats was transiently ligated for 2 h to induce cerebral infarction. The presence of cerebral infarction was evaluated via MRI 24 h after transient MCA occlusion, and SD rats with cerebral infarction were selected for subsequent study. The selected rats were blindly divided into four different groups, and each cell type was injected into the brain depending on the condition. Neurobehavioral functions were evaluated on a weekly basis using a beam-walking test and sticky-tape test. To confirm the effect of each condition on cerebral infarction, MRI was repeated 4 weeks after cerebral infarction. **b** MRI revealed that injecting ghMSCs 1 day after the induction of cerebral infarction significantly reduced infarct volume by more than 50%, and the effect of ghMSCs was much higher than that of hMSCs (by approximately 20%). This beneficial effect was almost completely blocked by anti-BP-4. **c** Neurobehavioral functions were markedly improved in the group treated with ghMSCs. In the beam-walking test, treatment with ghMSCs dramatically lowered the mean performance score to 0.6 ($P < 0.05$), which shows neurobehavioral improvement, at 3 weeks after cell injection, and this change was blocked with anti-BP-4. In the sticky-tape test, rats treated with ghMSCs reduced the time for the removal of sticky tape from their limbs to 40 s ($P < 0.01$), but this decrease disappeared when cotreated with anti-BP-4. Statistical analysis was performed using one-way ANOVA with post hoc analysis using Tukey's test among different groups and using paired t tests in the same group. (*, #, and \$, $P < 0.05$; ** ##, $P < 0.01$)

PD98059, an inhibitor of ERK, showed no effect (Fig. 2f). The PI3K/Akt pathway is involved in IGF-1 receptor (IGF-1R) signaling [21], and PPP, an inhibitor of IGF-1R, reduced the neuroprotective effect of ghMSC-CM ($P < 0.01$) (Fig. 2g). These results suggest that the IGF-1R pathway plays an important role in neuroprotection by IGFBP-4 in hypoxia-injured primary cortical neurons.

Akt Activation Via the IGF-1R Signaling Pathway by IGFBP-4 in ghMSC-CM

To examine Akt activation in IGFBP-4-mediated neuroprotection, the level of Akt phosphorylation induced by ghMSC-CM was investigated at different time points following OGD treatment. Phosphorylation was significantly enhanced by
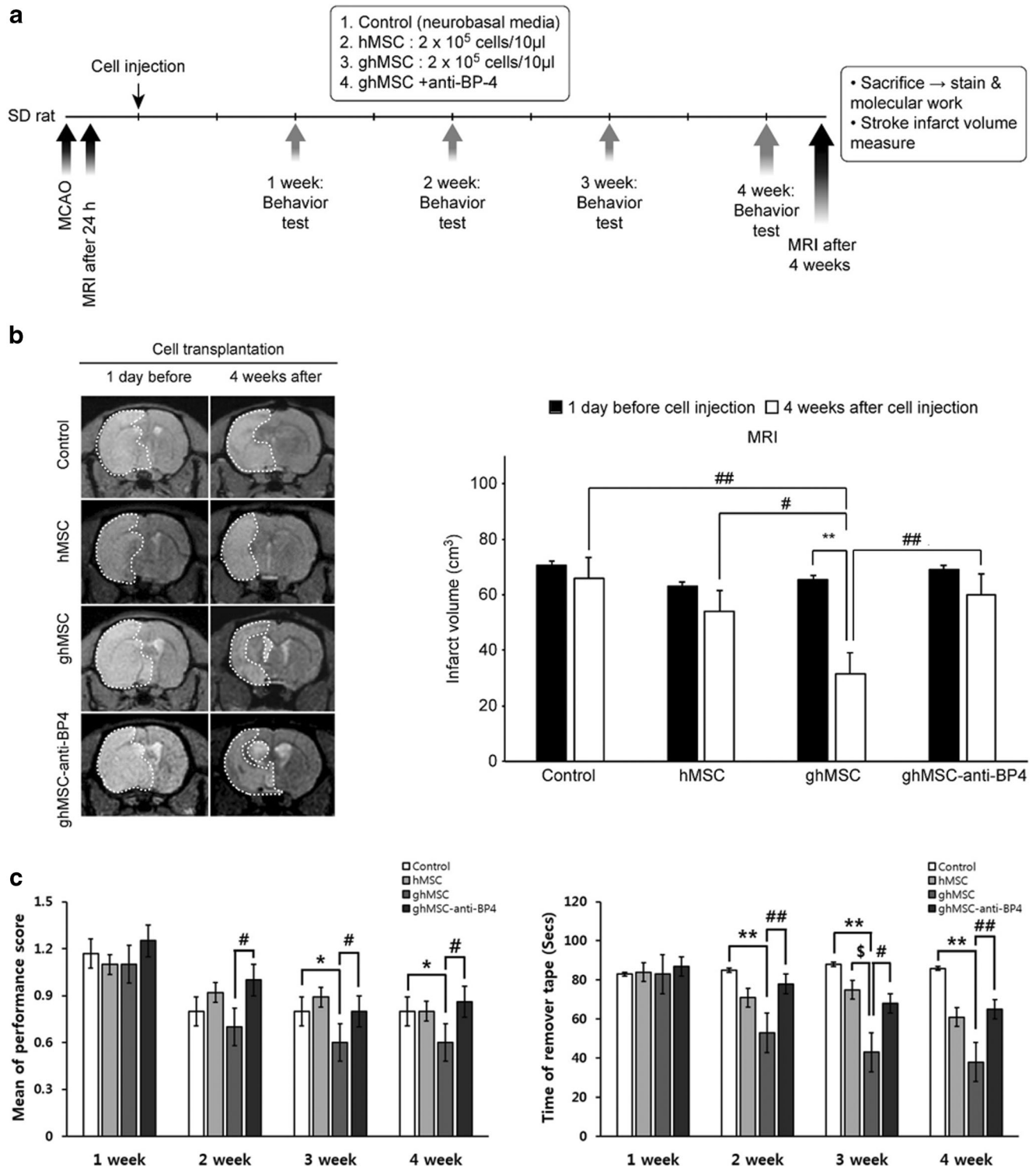
ghMSC-CM treatment for 30 min (Fig. 3a). First, the level of phosphorylated Akt (pAkt) after ghMSC-CM treatment was investigated following OGD treatment with or without anti-IGFBP-4 antibody incubation. The significantly increased pAkt levels in ghMSC-CM-treated primary cortical neurons after OGD treatment ($P < 0.01$) were dramatically reduced by anti-BP-4 incubation ($P < 0.05$) (Fig. 3b). In addition, ghMSC-CM preincubated with the IGF-1R inhibitor PPP significantly reduced the increase in pAkt levels induced by ghMSC-CM ($P < 0.001$) (Fig. 3c). These results suggest that IGFBP-4-induced activation of the Akt pathway via IGF-1R plays a crucial role in ghMSC-CM-mediated neuronal protection of OGD-damaged primary cortical neurons.

Bax Translocation Regulated by IGFBP-4

OGD-induced damage in cortical neurons dramatically increased mitochondrial Bax levels ($P < 0.001$) and dramatically decreased cytosolic Bax levels ($P < 0.001$), whereas ghMSC-CM treatment inhibited Bax translocation induced by apoptosis and significantly restored OGD-induced mitochondrial and cytosolic Bax to control levels ($P < 0.001$) (Fig. 3d, e). However, the effect of ghMSC-CM treatment was reversed by IGFBP-4 inhibition by anti-BP-4, Akt inhibition by wortmannin, and IGF-1R inhibition by PPP, which are involved in the IGF-1-dependent IGFBP-4 neuroprotective signaling pathway; this inhibition significantly enhanced mitochondrial Bax to OGD-damaged levels and reduced cytosolic Bax to the level observed with OGD treatment ($P < 0.001$) (Fig. 3d, e). These results indicate that Akt activation induced by IGFBP-4 promotes neuronal survival by inhibiting endogenous Bax translocation from the cytoplasm to the mitochondria.

Modulation of Extracellular IGF-1 and IGF-2 Levels by IGFBP-4

Considering that IGFBP-4 binds IGF-1 and IGF-2 with high affinity, and IGFBP-4 also regulates IGF-1 and/or IGF-2 action both in vitro and in vivo [22], it needed to be examined whether IGFBP-4 regulates extracellular IGF-1 and/or IGF-2 levels in OGD-damaged primary cortical neurons. ELISA showed that OGD treatment did not alter the extracellular levels of either IGF-1 or IGF-2. However, ghMSC-CM treatment after OGD significantly enhanced the level of extracellular IGF-1 compared with the control and OGD treatment ($P < 0.001$). However, this increase was abolished by IGFBP-4 inhibition (Fig. 3f). Similarly, ghMSC-CM treatment after OGD also increased the extracellular level of IGF-2 compared with the control ($P < 0.05$), which was reduced of control levels after IGFBP-4 inhibition ($P < 0.05$) (Fig. 3f). These results imply that IGFBP-4, which is highly expressed in ghMSCs, plays a crucial role in modulating extracellular IGF-1 and IGF-2 levels during neuronal protection against OGD-mediated injury.

Effect of ghMSCs on Cerebral Infarction

To assess the effect of ghMSCs in cerebral infarction, in vivo studies were performed under four different conditions (Fig. 3a). hMSCs (2×10^5 cells/10 μl), ghMSCs (2×10^5 cells/10 μl), ghMSCs (2×10^5 cells/10 μl) + anti-BP-4, and neurobasal media (as a control) were injected into the contralateral side of cerebral infarction, which was induced by transient middle cerebral artery occlusion (MCAo) in Sprague-Dawley (SD) rats. In the experiment to determine whether ghMSCs were able to protect the brain from cerebral infarction, MRI was regularly performed 1 day after surgery for transient MCAo and 4 weeks after cell injection. MRI showed that ghMSCs significantly and effectively reduced infarct volume by more than 50%, but this effect was almost completely blocked by combined injection with anti-BP-4 (Fig. 3b).

Neurobehavioral functions were also evaluated on a weekly basis after the injection of diverse types of stem cells depending on each condition. SD rats with cerebral infarction treated with ghMSCs showed marked improvements in the beam-walking test and sticky-tape test at 3 weeks and 2 weeks after the injection, respectively, compared with the other groups. In addition, these improvements disappeared upon combined treatment with anti-BP-4 (Fig. 4c).

IGFBP-4-Mediated Activation of the PI3K/Akt Pathway in the ghMSC-Protected Brain

Considering the results of the in vitro studies, the association between the protective effect of ghMSCs against cerebral infarction and the activation of the PI3K/Akt pathway by ghMSC-secreted IGFBP-4 should be confirmed. First, some signaling proteins involved in the PI3K/Akt pathway were investigated via immunohistochemistry and western blotting. Then, to determine whether the activation of the pathway is mediated by IGFBP-4 from ghMSCs, the same proteins were measured in the brains cotreated with ghMSCs and anti-BP-4.

According to immunohistochemical staining, phosphorylated Akt and Bcl-xl were significantly increased, and cytochrome c, Bax, and cleaved caspase-3 were remarkably decreased in the brain treated with ghMSCs (Fig. 5). However, these ghMSC-induced alterations were markedly blocked by anti-BP-4 (Fig. 5).

Western blotting also revealed that NeuN (a neuronal marker) and pAkt levels were increased in the brain implanted with ghMSCs and that Bax and cleaved caspase-9 were reduced following ghMSC injection (Fig. 6). These effects were blocked by combined treatment with anti-BP-4.

Discussion

Several studies have reported that the use of neurons or glia differentiated from hMSCs may be considered a

neuroreconstructive approach to treat neurological disorders [23]. In particular, the paracrine activity of hMSCs is considered an important effect for clinical trials [20, 24]. However, most clinical trials have thus far used only early-passage hMSCs lower than passage 5 despite the high cost because late-passage cells have much lower paracrine activity [25, 26]. This report is consistent with our in vivo results, in which transplanting late-passage hMSCs, namely, 11 through 14, had little effect on behavioral recovery (Fig. 4).

Thus, we optimized a method to boost the paracrine activity of late-passage hMSCs (> passage 5) via induction into ghMSCs (Fig. 1). Our results showed that ghMSCs significantly protected OGD-damaged primary cultured cortical neurons (Fig. 2). In vivo experiments also demonstrated that the brain was significantly protected from cerebral infarction and that neurobehavioral function was dramatically restored by ghMSC transplantation (Fig. 4). All these beneficial effects were clearly blocked by anti-BP-4 (Fig. 4). Akt signaling pathway components were activated, and antiapoptotic pathways in the brain were enhanced by ghMSC transplantation, and these beneficial alterations were significantly blocked by anti-BP-4 (Figs. 5 and 6). Taken together, our results demonstrate that ghMSCs, which were induced from late-passage hMSCs and release IGFBP-4, are a desirable cell source for treating ischemic stroke.
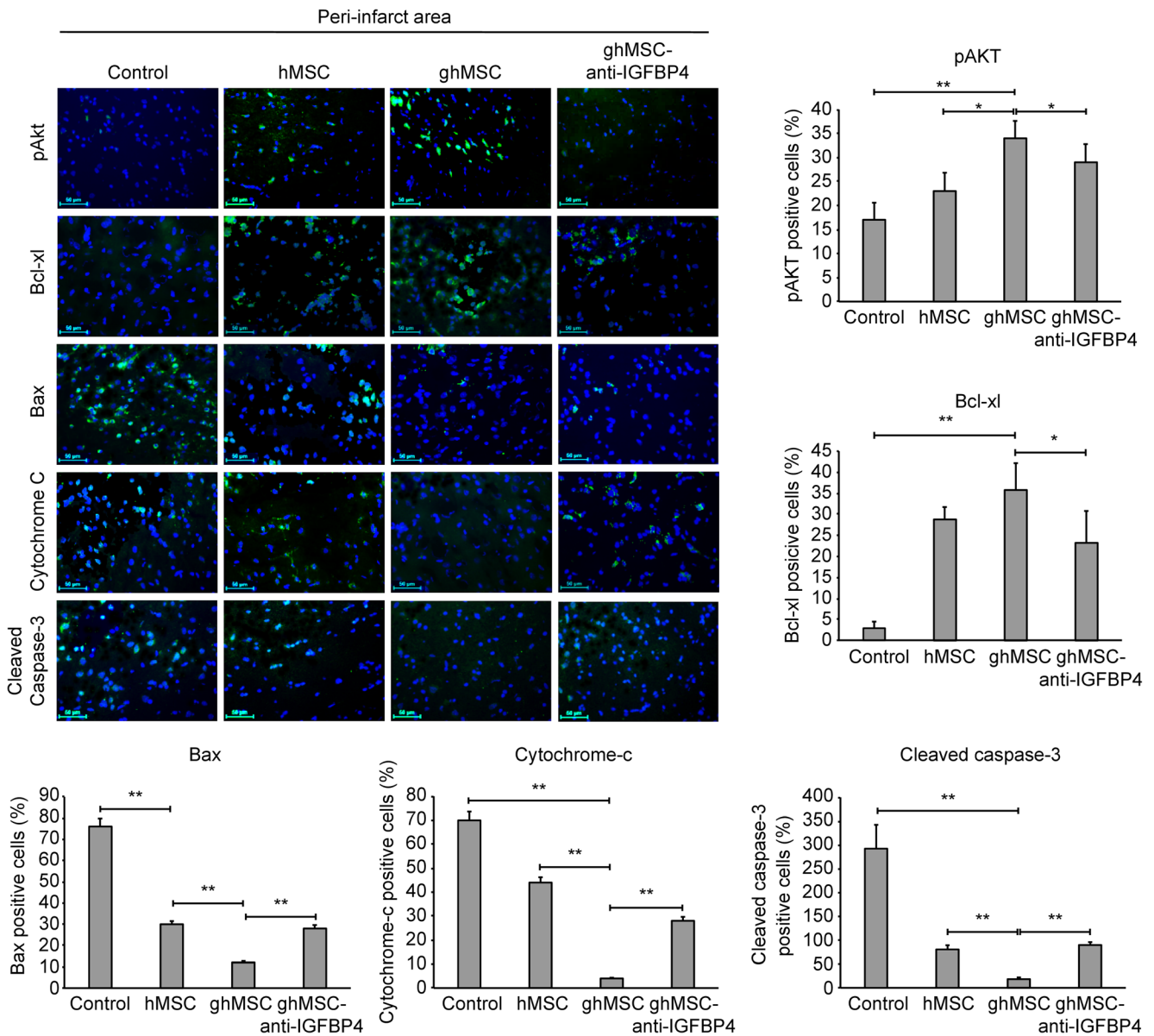
Fig. 5 IHC shows that IGFBP-4 plays key roles in the neuroprotective effect of ghMSCs against cerebral infarction. Immunohistochemical staining showed that ghMSCs increased phosphorylated Akt and Bcl-xl by more than two times ($P < 0.01$), while anti-BP-4 inhibited this effect. Cytochrome c, Bax, and cleaved caspase-3 were dramatically decreased to less than 10% ($P < 0.01$) following treatment with ghMSCs, and these reductions were reversed by anti-BP-4 ($P < 0.01$)
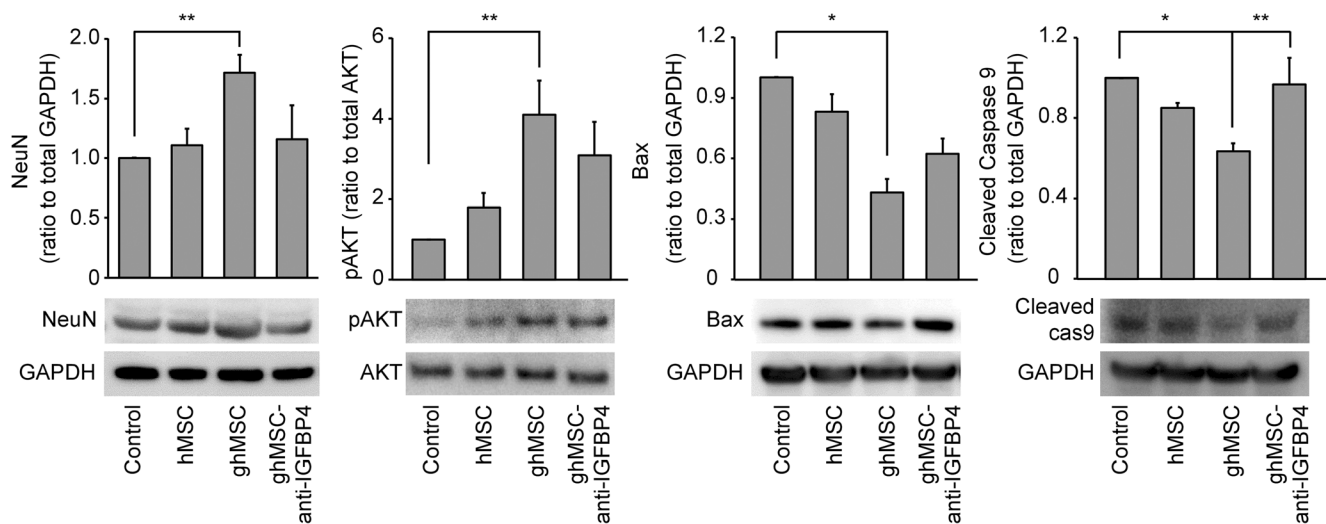
Fig. 6 Western blotting also shows that IGFBP-4 plays key roles in the neuroprotective effect of ghMSCs against cerebral infarction. Western blotting showed that NeuN, a neuronal marker, and phosphorylated Akt were upregulated more than twofold ($P < 0.05$) and that Bax and cleaved caspase-9 were downregulated following treatment with ghMSCs ($P < 0.01$). Statistical analysis was performed via one-way ANOVA with post hoc analysis using Tukey's test among different groups. (*$P < 0.05$; **$P < 0.01$)

In addition, the present study indicated for the first time that IGFBP-4 released from ghMSCs showed a neuroprotective effect in in vitro and in vivo ischemic stroke models. IGFBP-4, which is highly expressed in ghMSCs compared

Fig. 7 Graphical summary of the present study's conclusion
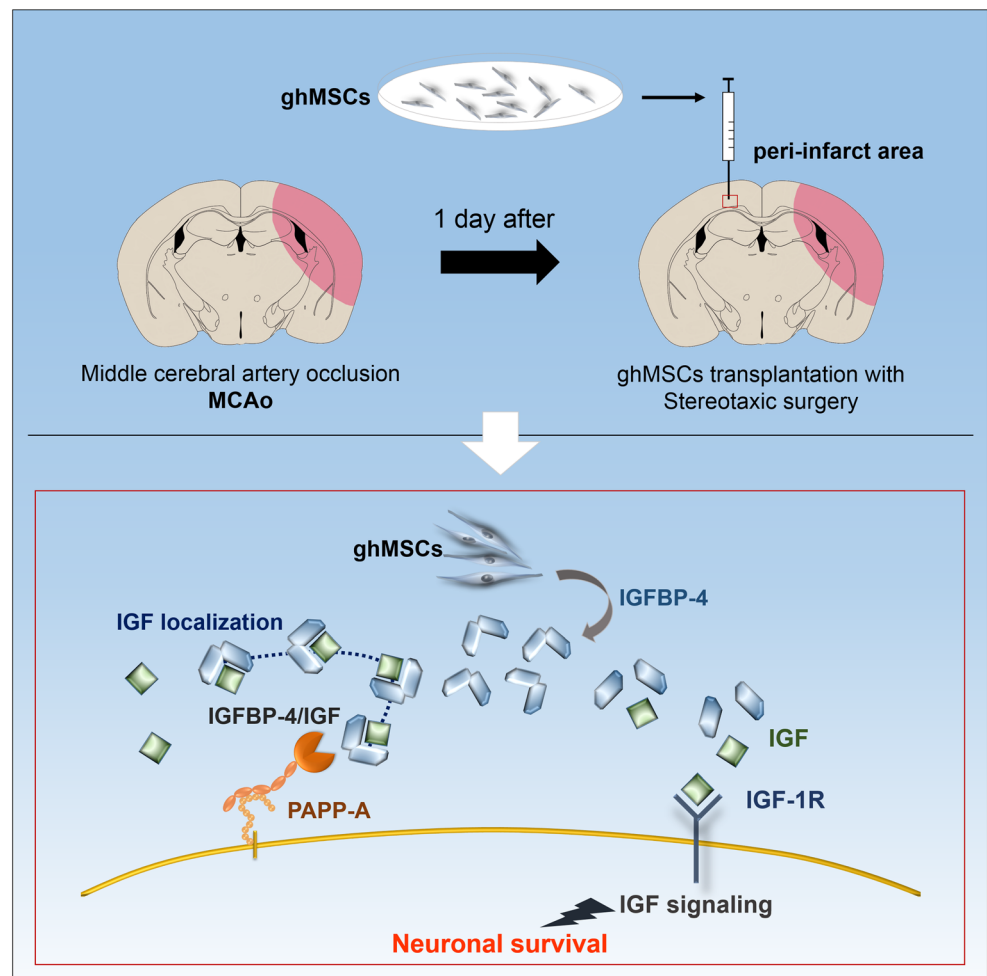
with hMSCs, enhanced neuronal survival in OGD-damaged cortical neurons (Fig. 2a, e) and reduced infarct volume induced by MCAo (Fig. 4a). According to ELISA, the IGFBP-4 concentration in ghMSC-CM was approximately only 8 ng/ml, relatively low compared with the neuroprotective working concentration (200 ng/ml) of rhBP-4 (Fig. 2c, e), indicating that endogenous IGFBP-4 showed neuroprotection with higher efficacy, probably because the endogenous protein is more stable due to posttranslational modification.

pAkt levels were dramatically increased following ghMSC-CM treatment in vitro (Fig. 3a) and by ghMSC transplantation in vivo (Figs. 5 and 6). Moreover, the increase in pAkt levels was clearly reversed by preincubating ghMSC-CM with anti-BP-4 or PPP (Fig. 3b, c) and by co-injecting anti-BP-4 with ghMSCs (Figs. 5 and 6), suggesting that IGFBP-4 enhances phosphorylation of Akt via IGF-1R signaling. Akt activation interrupts Bax translocation and thus mitochondria-mediated apoptosis [27], and the present results demonstrated that Bax translocation following OGD treatment was interrupted by IGFBP-4 in ghMSC-CM (Fig. 3d, e) and that Bax expression itself was decreased by IGFBP-4 from ghMSCs (Figs. 5 and 6). IGF-1R-mediated antiapoptotic signaling may be associated with extracellular levels of IGF-1 and IGF-2, which are modulated by IGFBP-4 released from ghMSCs (Fig. 3f).

IGFBP-4 was first identified and isolated based on its ability to inhibit IGF action. However, two different studies suggested that IGFBP-4 stimulates the effect of IGF-1 on neuronal survival by binding and localizing circulating IGF-1 to damaged neurons [28, 29]. IGFBP-4 stabilizes IGFs through the formation of an IGF/IGFBP-4 complex, which is proteolyzed by PAPP-A. PAPP-A, which was observed to be secreted from ghMSCs together with IGFBP-4 in the present study, is an IGF-dependent IGFBP-4 protease that cleaves IGFBP-4 and therefore increases local IGF bioavailability [30]. Free IGF binds IGF-1R and thereby potentiates antiapoptotic pathways by activating the PI3K/Akt and/or ERK pathway [21]. Other studies demonstrated that IGFBP-4 proteolysis is required for IGF-2 to enhance IGF-1 action and most IGF-2-dependent prenatal and postnatal growth [31, 32]. These studies indicated that IGF-2 is released from the IGF-2/IGFBP-4 complex through IGFBP-4 proteolysis induced by PAPP-A, which is located near the target cell surface. PAPP-A cell-surface binding is reversible, targeting the proximity to IGF-1R and thereby increasing the chance of IGF release by IGFBP-4 cleavage and stimulation of the receptor [19]. Similar to IGF-1, IGF-2 is a potent neuronal survival factor that binds to IGF-1R and activates signaling [33]. IGF-2/M6P-R, another IGF-2-binding receptor, was recently reported to be partially involved in neuroprotection in adult cortical neuronal cultures [34]. One study, however, suggested an antineuroprotective role of IGF-2 in the hypoxic-ischemic injured brain [35]. Thus, more studies on the neuroprotective

functions of IGF-2 are required. The present study suggested a new paradigm for IGFBP-4-mediated cellular survival in the nervous system. However, further studies are needed, particularly regarding the detailed mechanisms of IGFBP-4-mediated neuroprotection. For example, since IGFBP-4 cleavage plays a crucial role in modulating IGF activity both in vitro and in vivo, many studies have investigated the function of IGFBP-4 proteolytic fragments. However, the role of IGFBP-4 fragments in neuronal survival remains unclear, and further investigations are needed [22]. A few studies have suggested an IGF-1-independent effect of IGFBP-4 as a cardiogenic growth factor through the inhibition of canonical Wnt signaling, which enhanced cardiomyocyte differentiation both in vitro and in vivo [12, 36].

In conclusion, our study demonstrated that late-passage hMSCs can be efficiently induced into ghMSCs with better neuroprotective effects on ischemic stroke. Moreover, the results indicate that IGFBP-4 released from ghMSCs may serve as a key neuronal survival factor (Fig. 7). Using our approach, late-passage hMSCs could be utilized for cost-effective clinical trials.

References

1. Nguyen H, Zarriello S, Coats A, Nelson C, Kingsbury C, Gorsky A, Rajani M, Neal EG et al (2018) Stem cell therapy for neurological disorders: a focus on aging. Neurobiol Dis 126:85–104. https://doi.org/10.1016/j.nbd.2018.09.011

2. Maherali N, Sridharan R, Xie W, Utikal J, Eminli S, Arnold K, Stadtfeld M, Yachechko R et al (2007) Directly reprogrammed fibroblasts show global epigenetic remodeling and widespread tissue contribution. Cell Stem Cell 1(1):55–70. https://doi.org/10.1016/j.stem.2007.05.014

3. Okita K, Ichisaka T, Yamanaka S (2007) Generation of germline-competent induced pluripotent stem cells. Nature 448(7151):313–317. https://doi.org/10.1038/nature05934

4. Takahashi K, Yamanaka S (2006) Induction of pluripotent stem cells from mouse embryonic and adult fibroblast cultures by defined factors. Cell 126(4):663–676. https://doi.org/10.1016/j.cell.2006.07.024

5. Luo J, Zhao S, Wang J, Luo L, Li E, Zhu Z, Liu Y, Kang R et al (2018) Bone marrow mesenchymal stem cells reduce ureteral stricture formation in a rat model via the paracrine effect of extracellular vesicles. J Cell Mol Med 22(9):4449–4459. https://doi.org/10.1111/jcmm.13744

6. Hofer HR, Tuan RS (2016) Secreted trophic factors of mesenchymal stem cells support neurovascular and musculoskeletal therapies. Stem Cell Res Ther 7(1):131. https://doi.org/10.1186/s13287-016-0394-0

7. Yoon DS, Choi Y, Choi SM, Park KH, Lee JW (2015) Different effects of resveratrol on early and late passage mesenchymal stem cells through beta-catenin regulation. Biochem Biophys Res Commun 467(4):1026–1032. https://doi.org/10.1016/j.bbrc.2015.10.017

8. Ikegame Y, Yamashita K, Nakashima S, Nomura Y, Yonezawa S, Asano Y, Shinoda J, Hara H et al (2014) Fate of graft cells: what should be clarified for development of mesenchymal stem cell therapy for ischemic stroke? Front Cell Neurosci 8:322. https://doi.org/10.3389/fncel.2014.00322

9. Hwa V, Oh Y, Rosenfeld RG (1999) The insulin-like growth factor-binding protein (IGFBP) superfamily. Endocr Rev 20(6):761–787

10. Jeon HJ, Park J, Shin JH, Chang MS (2017) Insulin-like growth factor binding protein-6 released from human mesenchymal stem cells confers neuronal protection through IGF-1R-mediated signaling. Int J Mol Med 40(6):1860–1868. https://doi.org/10.3892/ijmm.2017.3173

11. Park HW, Lim MJ, Jung H, Lee SP, Paik KS, Chang MS (2010) Human mesenchymal stem cell-derived Schwann cell-like cells exhibit neurotrophic effects, via distinct growth factor production, in a model of spinal cord injury. Glia 58(9):1118–1132. https://doi.org/10.1002/glia.20992

12. Zhu W, Shiojima I, Ito Y, Li Z, Ikeda H, Yoshida M, Naito AT, Nishi J et al (2008) IGFBP-4 is an inhibitor of canonical Wnt signalling required for cardiogenesis. Nature 454(7202):345–349. https://doi.org/10.1038/nature07027

13. Kim YS, Yoo A, Son JW, Kim HY, Lee YJ, Hwang S, Lee KY, Lee YJ et al (2017) Early activation of phosphatidylinositol 3-kinase after ischemic stroke reduces infarct volume and improves long-term behavior. Mol Neurobiol 54(7):5375–5384. https://doi.org/10.1007/s12035-016-0063-4

14. Park HH, Lee KY, Park DW, Choi NY, Lee YJ, Son JW, Kim S, Moon C et al (2018) Tracking and protection of transplanted stem cells using a ferrocenecarboxylic acid-conjugated peptide that mimics hTERT. Biomaterials 155:80–91. https://doi.org/10.1016/j.biomaterials.2017.11.009

15. Son JW, Choi H, Yoo A, Park HH, Kim YS, Lee KY, Lee YJ, Koh SH (2015) Activation of the phosphatidylinositol 3-kinase pathway plays important roles in reduction of cerebral infarction by cilnidipine. J Neurochem 135(1):186–193. https://doi.org/10.1111/jnc.13254

16. Koh SH, Yoo AR, Chang DI, Hwang SJ, Kim SH (2008) Inhibition of GSK-3 reduces infarct volume and improves neurobehavioral functions. Biochem Biophys Res Commun 371(4):894–899. https://doi.org/10.1016/j.bbrc.2008.05.006

17. Urakawa S, Hida H, Masuda T, Misumi S, Kim TS, Nishino H (2007) Environmental enrichment brings a beneficial effect on beam walking and enhances the migration of doublecortin-positive cells following striatal lesions in rats. Neuroscience 144(3):920–933. https://doi.org/10.1016/j.neuroscience.2006.10.038

18. Sughrue ME, Mocco J, Komotar RJ, Mehra A, D'Ambrosio AL, Grobelny BT, Penn DL, Connolly ES, Jr. (2006) An improved test of neurological dysfunction following transient focal cerebral ischemia in rats. J Neurosci Methods 151 (2):83–89. doi:https://doi.org/10.1016/j.jneumeth.2005.04.023

19. Oxvig C (2015) The role of PAPP-A in the IGF system: location, location, location. J Cell Commun Signal 9(2):177–187. https://doi.org/10.1007/s12079-015-0259-9

20. Torrente D, Avila MF, Cabezas R, Morales L, Gonzalez J, Samudio I, Barreto GE (2014) Paracrine factors of human mesenchymal stem cells increase wound closure and reduce reactive oxygen species production in a traumatic brain injury in vitro model. Hum Exp Toxicol 33(7):673–684. https://doi.org/10.1177/0960327113509659

21. LeRoith D, Werner H, Beitner-Johnson D, Roberts CT Jr (1995) Molecular and cellular aspects of the insulin-like growth factor I receptor. Endocr Rev 16(2):143–163

22. Mazerbourg S, Callebaut I, Zapf J, Mohan S, Overgaard M, Monget P (2004) Up date on IGFBP-4: regulation of IGFBP-4 levels and functions, in vitro and in vivo. Growth Hormon IGF Res 14(2):71–84. https://doi.org/10.1016/j.ghir.2003.10.002

23. Chang YK, Chen MH, Chiang YH, Chen YF, Ma WH, Tseng CY, Soong BW, Ho JH et al (2011) Mesenchymal stem cell transplantation ameliorates motor function deterioration of spinocerebellar ataxia by rescuing cerebellar Purkinje cells. J Biomed Sci 18:54. https://doi.org/10.1186/1423-0127-18-54

24. Boido M, Piras A, Valsecchi V, Spigolon G, Mareschi K, Ferrero I, Vizzini A, Temi S et al (2014) Human mesenchymal stromal cell transplantation modulates neuroinflammatory milieu in a mouse model of amyotrophic lateral sclerosis. Cytotherapy 16(8):1059–1072. https://doi.org/10.1016/j.jcyt.2014.02.003

25. Bang OY, Lee JS, Lee PH, Lee G (2005) Autologous mesenchymal stem cell transplantation in stroke patients. Ann Neurol 57(6):874–882. https://doi.org/10.1002/ana.20501

26. Mazzini L, Ferrero I, Luparello V, Rustichelli D, Gunetti M, Mareschi K, Testa L, Stecco A et al (2010) Mesenchymal stem cell transplantation in amyotrophic lateral sclerosis: a phase I clinical trial. Exp Neurol 223(1):229–237

27. Tsuruta F, Masuyama N, Gotoh Y (2002) The phosphatidylinositol 3-kinase (PI3K)-Akt pathway suppresses Bax translocation to mitochondria. J Biol Chem 277(16):14040–14047. https://doi.org/10.1074/jbc.M108975200

28. Kummer JL, Zawada WM, Freed CR, Chernausek SD, Heidenreich KA (1996) Insulin-like growth factor binding proteins in fetal rat mesencephalic cultures: regulation by fibroblast growth factor and insulin-like growth factor I. Endocrinology 137(8):3551–3556

29. Nordqvist A-CS, Von Holst H, Holmin S, Sara V, Bellander B-M, Schalling M (1996) Increase of insulin-like growth factor (IGF)-1, IGF binding protein-2 and− 4 mRNAs following cerebral contusion. Mol Brain Res 38(2):285–293

30. Zhou R, Diehl D, Hoeflich A, Lahm H, Wolf E (2003) IGF-binding protein-4: biochemical characteristics and functional consequences. J Endocrinol 178(2):177–193

31. Conover CA, Durham SK, Zapf J, Masiarz FR, Kiefer MC (1995) Cleavage analysis of insulin-like growth factor (IGF)-dependent IGF-binding protein-4 proteolysis and expression of protease-resistant IGF-binding protein-4 mutants. J Biol Chem 270(9):4395–4400

32. Ning Y, Schuller AG, Conover CA, Pintar JE (2008) Insulin-like growth factor (IGF) binding protein-4 is both a positive and negative regulator of IGF activity in vivo. Mol Endocrinol 22(5):1213–1225. https://doi.org/10.1210/me.2007-0536

33. Cianfarani S (2012) Insulin-like growth factor-II: new roles for an old actor. Front Endocrinol (Lausanne) 3:118. https://doi.org/10.3389/fendo.2012.00118

34. Martin-Montanez E, Pavia J, Santin LJ, Boraldi F, Estivill-Torrus G, Aguirre JA, Garcia-Fernandez M (2014) Involvement of IGF-II receptors in the antioxidant and neuroprotective effects of IGF-II on adult cortical neuronal cultures. Biochim Biophys Acta 1842(7):1041–1051. https://doi.org/10.1016/j.bbadis.2014.03.010

35. Guan J, Williams CE, Skinner SJM, Mallard EC, Gluckman PD (1996) The effects of insulin-like growth factor (IGF)-1, IGF-2, and des-IGF-1 on neuronal loss after hypoxic-ischemic brain injury in adult rats: evidence for a role for IGF binding proteins. Endocrinology 137(3):893–898

36. Xue Y, Yan Y, Gong H, Fang B, Zhou Y, Ding Z, Yin P, Zhang G et al (2014) Insulin-like growth factor binding protein 4 enhances cardiomyocytes induction in murine-induced pluripotent stem cells. J Cell Biochem 115(9):1495–1504. https://doi.org/10.1002/jcb.24804